Biochemical and Biophysical Research Communications 421 (2012) 763–767

Contents lists available at SciVerse ScienceDirect

Biochemical and Biophysical Research Communications

journal homepage: www.elsevier.com/locate/ybbrc

Intracellular trafficking of superparamagnetic iron oxide nanoparticles conjugated with TAT peptide: 3-dimensional electron tomography analysis

Baiju G. Nair, Takahiro Fukuda, Toru Mizuki, Tatsuro Hanajiri, Toru Maekawa *

Bio-Nano Electronics Research Centre, Toyo University, Saitama 350-8585, Japan

ARTICLE INFO

Article history:
Received 28 March 2012
Available online 21 April 2012

Keywords:
Nanoparticles
Internalisation
Cell penetrating peptides
Endocytic pathways
Transmission electron microscopy
3-D tomography

ABSTRACT

Internalisation of nanoparticles conjugated with cell penetrating peptides is a promising approach to various drug delivery applications. Cell penetrating peptides such as transactivating transcriptional activator (TAT) peptides derived from HIV-1 proteins are effective intracellular delivery vectors for a wide range of nanoparticles and pharmaceutical agents thanks to their amicable ability to enter cells and minimum cytotoxicity. Although different mechanisms of intracellular uptake and localisation have been proposed for TAT conjugated nanoparticles, it is necessary to visualise the particles on a 3-D plane in order to investigate the actual intracellular uptake and localisation. Here, we study the intracellular localisation and trafficking of TAT peptide conjugated superparamagnetic ion oxide nanoparticles (TAT-SPIONs) using 3-D electron tomography. 3-D tomograms clearly show the location of TAT-SPIONs in a cell and their slow release from the endocytic vesicles into the cytoplasm. The present methodology may well be utilised for further investigations of the behaviours of nanoparticles in cells and eventually for the development of nano drug delivery systems.

1. Introduction

Nanoparticles internalised in cells can be utilised in various biomedical areas such as hyperthermia, drug release, imaging and gene silencing [1–3]. To make the above operations successful, nanoparticles need to enter the cells and stay inside for a period of time, which in particular projects an important aspect of nanodrug delivery systems [4]. It is well known that nanoparticles can enter a cell via different methods; i.e., non specific uptake by endocytosis, direct injection of nanomaterials, electroporation and specifically targeted uptake of nanomaterials functionalised with various targeting moieties. Among the above methods, nanoparticles conjugated with specific ligands are highly promising for selective nanodrug delivery systems [5]. Cell penetrating peptide (CPP) is supposed to be one of the best ligands to improve active internalisation of nanoparticles into a target cell [6]. CPPs in general translocate efficiently across cell membranes, but the exact mechanism of the cell penetrating activity is still under investigation [7]. CPPs such as transactivating transcriptional activator (TAT) peptide derived from HIV can transport a large number of nanoparticles into a mammalian cell cytoplasm avoiding the normal endocytic pathways through the penetration of the cell membrane [8]. Complete lack of specificity of TAT peptides used to be a solemn matter of concern for targeting a cancer cell, but a selective internalisation of nanoparticles into a cancer cell was successfully performed by combining TAT peptides with cell targeting peptides (CTPs) [9]. This kind of combined peptides can be utilised for the internalisation of an enormous amount of nanoparticles into cells and are also useful for various intracellular manipulation studies [10]. Internalisation of a massive number of nanoparticles into a target cell and their escape from the normal endocytic pathways are attractive features particularly for nano drug delivery systems [11]. Most of the studies on the internalisation of nanoparticles are based on the confocal and flow cytometry analyses. However, a complete visualisation of intracellular trafficking of nanoparticles using the above optical methods is quite difficult due to the high electrostatic interaction between nanoparticles and the surface of cells, which often leads to wrong interpretations of the data [12]. Transmission electron microscopic (TEM) studies support the identification and characterisation of nanoparticles internalised in a cell [13–16]. In the case of 2-D TEM images, however, it is extremely difficult to differentiate whether the nanoparticles are present in the resin or lying on the surface of cell sections without being internalised, or whether the nanoparticles are distributed in the 3-D volume of the section or not. 3-D electron tomography (ET) is a well-established technique in biological sciences. In 3-D ET, the specimen is rotated around an axis at a range of tilt angles perpendicular to the electron beam and multiple 2-D projection images of a 3-D sample are recorded. Finally, high resolution 3-D images are constructed from a set of 2-D images [17]. The 3-D structures of organelles and macromolecular assemblies [18] and the molecular organisation of the cytoplasm in thin sections of

* Corresponding author.
E-mail address: maekawa@toyo.jp (T. Maekawa).

0006-291X/$ - see front matter © 2012 Elsevier Inc. All rights reserved.
http://dx.doi.org/10.1016/j.bbrc.2012.04.080

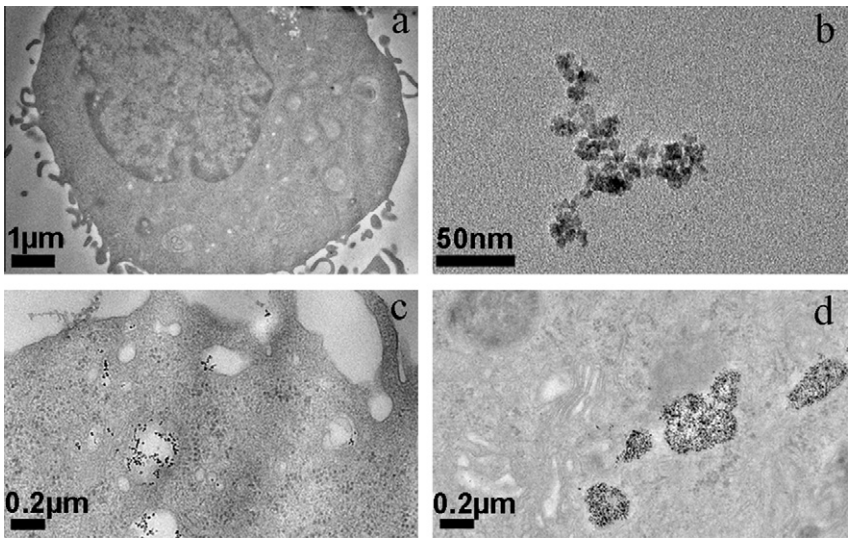

Fig. 1. TEM images of superparamagnetic ion oxide nanoparticles (SPIONs) in a glioma cell. (A) Glioma cell (Control); (B) Clusters composed of HIV-1 TAT peptide conjugated SPIONs (TAT-SPIONs); (C) Bare SPIONs in a glioma cell; (D) TAT-SPIONs in a glioma cell. A large amount of TAT- SPIONs were internalised in vesicles of the glioma cell. Although bare SPIONs were also internalised in the cell, the quantity was much less compared to the TAT-SPIONs.

cells [19] were visualised by 3-D ET. The structure of a virus based on their outer layer glycoprotein spikes, interior nuclear caspid and tegument was also visualised [20]. 3-D ET also augmented the study on pathways exhibited by viruses at different stages of infection focusing on the nano ecology of the protein spikes present on the viral envelop [21]. For instance, the interaction between SIV/HIV-1 viruses and the surface of cells and the entry of these viruses into cells were clearly visualised using 3-D ET [22]. Moreover, the life cycle of a virus in a host cell and related intracellular pathways including endocytic pathways and nuclear entry at different stages of viral infection were successfully visualised by 3-D ET [23]. Interestingly, each ligand conjugated nanoparticle can be viewed as a miniature form of a virus [24,25] and the successful visualisation of the intracellular activities of viruses in a host cell by 3-D ET can be utilised as an inspiring tool for the visualisation of nanoparticles interacting with cells. Intracellular uptake and related localisation of nanomaterials such as carbon nanotubes and fullerenes without any modification with ligands were visualised by 3-D ET [26,27]. In the present study, we analysed the intracellular localisation and trafficking of HIV-1 TAT peptide conjugated superparamagnetic iron oxide nanoparticles (TAT-SPIONs) in a glioma cell by 3-D ET. We suppose that the present study gives more insight into the interactions between nanoparticles and cells and may encourage further investigations of the effect of the type of ligands and the size and material of nanoparticles on the intracellular trafficking of nanoparticles using 3-D ET.

2. Materials and methods

2.1. Preparation of TAT-SPIONs

Commercially available superparamagnetic iron oxide nanoparticles (nanomag®-D – spio PEG COOH, Micromod, Germany) of 50 nm average diameter coated with PEG were used for the experimental studies. An 11-mer HIV-1 TAT peptide (YGRKKRRQRRR) (Anaspec, USA) was conjugated with SPIONs using the carbodiimide coupling chemistry [28]. 50 µl of SPIONs were treated with 250 mM 1-ethyl-3-[3-dimethylaminopropyl] carbodiimide hydrochloride (EDC) and 100 mM *N*-hydroxysulfosuccinimide (S-NHS) (Pierce, Thermo Scientific, USA) in MES buffer of pH 5.5 (BupH MES, Thermo Scientific, USA) and incubated for 15 min. Then, 1 mg of peptide in 100 µl of 50 mM sodium tetraborate (Wako Pure Chemical, Japan) containing 100 mM sodium chloride was added to the carboxyl group activated SPIONs and the mixture was kept at 20 °C for 4 h. After the conjugation, free peptides were separated by centrifugal filters (Nanosep, 100K, Pall Corporation, USA). Peptide conjugated nanoparticles were washed three times with MES buffer and were resuspended in fresh PBS for cell interaction studies.

2.2. Cell internalisation protocols

Human glioblastoma (U251, JCRB, Japan) were grown on a tissue culture flask with 10% heat inactivated fetal bovine serum and 1% antibiotics in MEM (Sigma–Aldrich, USA) and after three passages, cells were maintained at 1×10^5 cells ml^{-1}. For internalisation studies, cells were grown on 60 mm culture plates to reach confluence of approximately 60%. Next, cells were washed with Dulbecco's PBS (Sigma–Aldrich, USA) and incubated with 25 µl of TAT peptide conjugated SPIONs or bare SPIONs in the culture medium for 4 h.

2.3. 3-D electron tomography studies

Glioma cells incubated with either TAT-SPIONs or bare SPIONs were washed twice with PBS to remove any residual particles on the cells. Samples for TEM observations were prepared according to the protocol mentioned elsewhere [29]. After cutting the resin embedded samples in 70–80 nm thickness with an ultramicrotome using a 45° wedge angle diamond knife (Lieca Ultracut, Germany), the sections were put on a 300 mesh copper grid and observed by a TEM (JEM 2100, JEOL, Japan) at 120–200 kV. 3-D ET was conducted on the same cell sections as those observed in 2-D electron microscopy. The cell specimen was tilted at an angle from −60 to +60 at 1° increment for better resolution and electron micrographs were taken by a slow scan CCD camera. 3-D reconstruction of each 2-D image was carried out by composer and visualiser application software (TEMOgraphy™, System in Frontier Inc., Japan). Various quantitative structural analyses of cells were carried out by zooming, rotating, panning and tilting the 3-D images to understand the diverse behaviours of the molecular assemblies in a cell [30]. Finally, slicing of 3-D images on XZ and YZ planes was carried

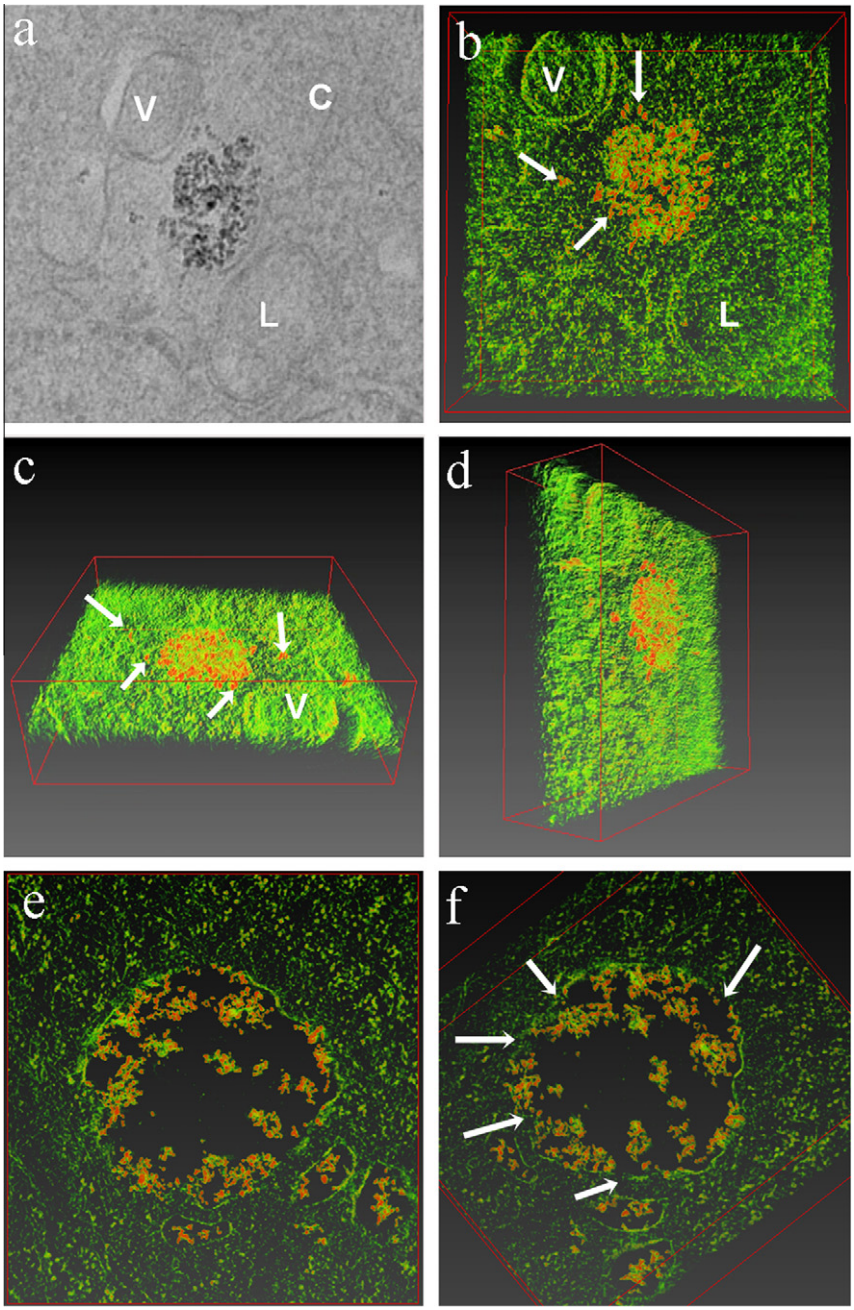

Fig. 2. Localisation and endosomal escape of TAT- SPIONs in a glioma cell. (A) TEM image of TAT-SPIONs internalised in a glioma cell. C, V and L represent, respectively, cytoplasm, vacuole and lysosome. (B),(C),(D) 3-D electron tomograms. TAT-SPIONs are represented by red and TAT-SPIONs escaping from the vacuole into the cytoplasm are indicated by arrows. A 3-D movie corresponding to (B), (C) and (D) is given in the Supplementary Information. The scale bars indicated in the *x*-axis, *y*-axis and *z*-axis represent, respectively, 628.74, 628.74 and 214.20 nm. (E),(F) 3-D electron tomograms. A 3-D movie corresponding to (E) and (F) is also given in the Supplementary Information. TAT-SPIONs are localised inside a vacuole and their partial escape into the cytoplasm are clearly visualised. The scale bars in the *x*-axis, *y*-axis and *z*-axis represent, respectively, 1745.22, 1130.42 and 242.94 nm. (For interpretation of the references to colour in this figure legend, the reader is referred to the web version of this article.)

out to observe the localisation of nanoparticles in horizontal and vertical cross-sections of cells.

3. Results and discussion

First of all, TAT-SPIONs were monodispersed in water and the average hydrodynamic diameter of each particle was 70 nm. TEM images of glioma cells and TAT-SPIONs are shown in Fig. 1. Clusters were formed by TAT-SPIONs under vacuum conditions (see Fig. 1(B)) although they were monodispersed in water as mentioned. We found that a large amount of TAT-SPIONs were internalised in vesicles in the glioma cell (see Fig. 1(D)), whereas the control studies using bare SPIONs without any conjugation with the TAT peptide also showed internalisation of nanoparticles forming endocytic vesicles inside the cell, but the amount of nanoparticles internalised in the cell was much smaller compared to TAT-SPIONs (see Fig. 1(C), (D)). EDS mappings exposed the presence of iron in all of the internalised nanoparticles in the cells (see the Supplementary Information for the EDS mappings). In the previous study using 2-D electron microscopy, TAT peptide conjugated gold nanoparticles breached the vacuole membrane to reach different

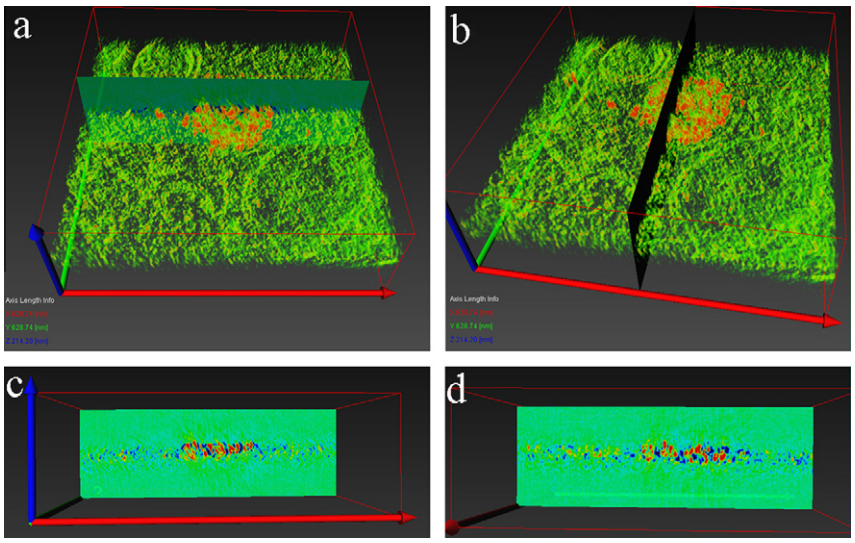

Fig. 3. Slicing of a tomogram on two orthogonal planes. (A) Slicing on an XZ plane. (B) Slicing on an XY plane. (C) Cross-sectional image corresponding to (A). (D) Cross-sectional image corresponding to (B). The scale bars indicated in red (*x*-axis), in green (*y*-axis) and in blue (*z*-axis) represent, respectively, 628.74, 628.74 and 214.20 nm. TAT-SPIONs indicated in red were internalised in a vacuole and some of them moved out of the vacuole in horizontal directions. (For interpretation of the references to colour in this figure legend, the reader is referred to the web version of this article.)

cell organelles [31], while we observed by the present 2-D electron microscopy that TAT-SPIONs were mainly accumulated in the endocytic vesicles and started escaping into cytosol. To confirm that the above interpretation is correct, we obtained snapshots of electron tomograms of several endocytotic vesicles filled with TAT-SPIONs. Fig. 2 shows snapshots of 3-D tomograms. The localisation of TAT-SPIONs inside a vacuole and their partial escape into the cytoplasm before proceeding into lysosomes or a complete endocytotic pathway are clearly visualised in Fig. 2(B)–(D), where red represents low transmission intensity areas of electron beams; i.e., TAT-SPIONs (see also the Supplementary Information for a 3-D movie created from the above 3-D tomograms). This suggests that endocytosis is the main mechanism of the cell internalisation of CPP-nanoparticle conjugates even though CPP and nanoparticles can exhibit different modes of the cell internalisation process [32]. Quite a few different mechanisms of the escape and release of TAT-nanoparticle conjugates from the endocytic vesicle into the cytoplasm have been proposed [33]. To elucidate the above equivocal concept or mechanism, we carried out 3-D ET analysis of an endocytic vesicle filled with a small number of TAT-SPIONs (see Fig. 2(E), (F) and the Supplementary Information for the 3-D movie corresponding to Fig. 2(E), (F)). It is clearly visualised that the endocytic vesicle was destabilised by passages or pores formed in the membrane, through which TAT-SPIONs translocated into the cytoplasm. The destabilisation of the vesicle might have been caused by the stress imposed on the internal membrane by TAT-SPIONs internalised in the vesicle [34]. Horizontal and vertical cross-sections of a tomogram on XZ and YZ planes are shown in Fig. 3. It is clearly shown that some of the TAT-SPIONs, which had accumulated in a vacuole, moved out into the cytoplasm.

We used TAT-SPIONs as model particles and carried out 3-D ET analysis of internalisation of TAT-SPIONs in a cell 4 h after the incubation. Slicing of tomograms at a range of several nanometres on different planes, which is practically impossible in the case of TEM visualisations using an ultramicrotome, can give more detailed information about the internal morphology of a cell, which is another highlight of 3-D ET [35]. We believe that 3-D ET analysis of intracellular trafficking of therapeutic nanoparticles conjugated with a wide range of targeting ligands will encourage further studies on nano drug delivery systems. We will be investigating particles' internalisation in a cell and escape into the cytoplasm in more detail changing the ligand and the time interval after the incubation. The present 3-D ET approach to the understanding of the mechanisms of internalisation of nanopartciles in cells may encourage further investigations of drug delivery, release and therapeutic processes occurring in a cell. It may be possible to target, manipulate and visualise specific organelles in a cell by using superparamagnetic nanoparticles conjugated with specific ligands and external magnetic fields [36,37].

Acknowledgments

Part of the present study has been supported by a Grant for the Strategic Development of Advanced Science and Technology S1101017 organised by the Ministry of Education, Culture, Sports, Science and Technology (MEXT), Japan, since April 2011.

Appendix A. Supplementary data

Supplementary data associated with this article can be found, in the online version, at http://dx.doi.org/10.1016/j.bbrc.2012.04.080.

References

[1] T. Kobayashi, Cancer hyperthermia using magnetic nanoparticles, Biotechnol. J. 6 (2011) 1342–1347.
[2] C. Wang, L. Cheng, Z. Liu, Drug delivery with upconversion nanoparticles for multifunctional targeted cancer cell imaging and therapy, Biomaterials 32 (2011) 1110–1120.
[3] R. Bartz, H. Fan, J. Zhang, N. Innocent, C. Cherrin, S.C. Beck, Y. Pie, A. Momose, V. Jadhav, D.M. Tellers, F. Meng, L.S. Crocker, L. Sepp-Lorenzino, S.F. Barnett, Effective siRNA delivery and target mRNA degradation using an amphipathic peptide to facilitate PH- dependent endosomal escape, Biochem. J. 435 (2011) 475–487.
[4] H. Hillaireau, P. Couvreur, Nanocarriers' entry into the cell: relevance to drug delivery, Cell. Mol. Life Sci. 66 (2009) 2873–2896.
[5] J. Gao, B. Xu, Application of nanomaterials inside cells, Nano Today 4 (2009) 37–51.
[6] M.C. Morris, S. Deshayers, F. Heitz, G. Divita, Cell-penetrating peptides: from molecular mechanism to therapeutics, Biol. Cell. 100 (2008) 201–217.
[7] N.W. Schmidt, A. Mishra, G.H. Lai, G.C.L. Wong, Arginine-rich cell penetrating peptides, FEBS Lett. 584 (2010) 1806–1813.
[8] V.P. Torchilin, R. Rammohan, V. Weissig, T.S. Levchenko, TAT peptide on the surface of liposomes affords their efficient intracellular delivery even at low temperature and in the presence of metabolic inhibitors, Proc. Natl. Acad. Sci. U.S.A. 98 (2009) 8786–8791.
[9] J. Jung, A. Solanki, K.A. Memoli, K. Kamei, H. Kim, M.A. Drahl, L.J. Williams, H.R. Tseng, K.B. Lee, Selective inhibition of human brain tumor cells through

multifunctional quantum-dot-based siRNA delivery, Angew. Chem. Int. Ed. 49 (2010) 103–107.
[10] V.P. Torchilin, Tat peptide-mediated intracellular delivery of pharmaceutical nanocarriers, Adv. Drug Deliv. Rev. 60 (2000) 548–558.
[11] A. Chugh, F. Eudes, Y.S. Shim, Cell-penetrating peptides: nanocarrier for macromolecule delivery in living cells, IUBMB Life 62 (2010) 183–193.
[12] T.G. Iversen, T. Skotland, K. Sandvig, Endocytosis and intracellular transport of nanoparticles: present knowledge and need for future studies, Nano Today 6 (2011) 176–185.
[13] C. Wilhelm, F. Gazeau, J. Roger, J.C. Pons, Interaction of anionic superparamagnetic nanoparticles with cells: kinetic analyses of membrane adsorption and subsequent internalization, Langmuir 18 (2002) 8148–8155.
[14] R. Shukla, V. Bansal, M. Chaudhar, A. Basu, R.R. Bhonde, M. Sastry, Biocompatibility of gold nanoparticles and their endocytotic fate inside the cellular compartment: a microscopic overview, Langmuir 21 (2005) 10644–10654.
[15] A.E. Porter, M. Gass, K. Muller, J.N. Skipper, P.A. Midgley, M. Wellad, Direct imaging of single-walled carbon nanotubes in cells, Nat. Nanotechnol. 2 (2007) 713–717.
[16] J. Yu, H. Zhao, L. Ye, H. Yang, S. Ku, N. Yang, N. Xiao, Effect of surface functionality of magnetic silica nanoparticles on the cellular uptake by glioma cells *in vitro*, J. Mater. Chem 19 (2009) 1265–1270.
[17] O. Medalia, I. Weber, A.S. Frangakis, D. Nicastro, G. Gerisch, W. Baumeister, Macromolecular architecture in eukaryotic cells visualized by cryoelectron tomography, Science 298 (2002) 1209–1213.
[18] K. Ben-Harush, T. Maimon, I. Patla, E. Villa, O. Medalia, Visualizing cellular processes at the molecular level by cryo-electron tomography, J. Cell Sci. 1 (2010) 7–12.
[19] W. Baumeister, Electron tomography: towards visualizing the molecular organization of the cytoplasm, Curr. Opin. Struct. Biol. 12 (2002) 679–684.
[20] K. Grünewald, P. Desai, D.C. Winkler, J.B. Heymann, D.M. Belnap, W. Baumeister, A.C. Steven, Three-dimensional structure of herpes simples virus form cryo-electron tomography, Science 302 (2003) 1396–1398.
[21] K. Iwasaki, T. Omura, Electron tomography of the supramolecular structure of virus-infected cells, Curr. Opin. Struct. Biol. 20 (2010) 632–639.
[22] R. Sougrat, R. Sougrat, A. Bartesaghi, J.D. Lifson, A.E. Bennett, J.W. Bess, D.J. Zabransky, S. Subramaniam, Electron tomography of the contact between T cells and SIV/HIV-1: implications for viral entry, PLoS Pathog. 5 (2007) e63.
[23] L. Peng, S. Ryazantsev, R. Sun, Z.H. Zhou, Three-dimensional visualization of gammaherpesvirus life cycle in host cells by electron tomography, Structure 13 (2010) 47–58.
[24] H. Yuan, C. Huang, S. Zhang, Virus-inspired design principles of nanoparticle-based bioagents, PLoS One 5 (2010) e13495.
[25] R. Vácha, F.J. Martinez-Veracoechea, D. Frenkel, Receptor-mediated endocytosis of nanoparticles of various shapes, Nano Lett. 11 (2011) 5391–5395.
[26] A.E. Porter, M. Gass, K. Muller, J.N. Skipper, P.A. Midgley, M. Wellad, Visualizing the uptake of C_{60} to the cytoplasm and nucleus of human monocyte-derived macrophage cells using energy-filtered transmission electron microscopy and electron tomography, Environ. Sci. Technol. 41 (2007) 3012–3017.
[27] K.T. Al-Jamal, H. Nerl, K.H. Müller, H. Ali-Boucetta, S. Li, P.D. Haynes, J.R. Jinschek, M. Prato, A. Bianco, K. Kostarelos, A.E. Porter, Cellular uptake mechanisms of functionalized muti-walled carbon nanotubes by 3-D electron tomography imaging, Nanoscale 3 (2011) 2627–2635.
[28] G.T. Hermanson, Bioconjugate Techniques, second ed., Academic press, USA, 2008.
[29] M.A. Schrand, J.J. Schlager, L. Dai, S.M. Husain, Preparation of cells for assessing ultra structural localization of nanoparticles with transmission electron microscopy, Nat. Protoc. 5 (2010) 744–757.
[30] R. Mclntosh, D. Nicastro, D. Mastronarde, New views of cells in 3D: an introduction to electron tomography, Trends Cell Biol. 15 (2005) 43–51.
[31] Z. Krpetić, S. Saleemi, I.A. Prior, V. Sée, R. Qureshi, M. Brust, Negotiation of intracellular membrane barriers by TAT-modified gold nanoparticles, ACS Nano 5 (2011) 5195–5201.
[32] S. Trabulo, A. Cardoso, M. Mano, M.C. Pedroso de Lima, Cell-penetrating peptides-mechanism of cellular uptake and generation of delivery systems, Pharmaceuticals 3 (2010) 961–993.
[33] A.K. Varkouhi, M. Scholte, G. Storm, H.J. Haisma, Endosomal escape pathways for delivery of biologicals, J. Control. Release 10 (2011) 220–228.
[34] A. Mishra, G.H. Lai, N.W. Schmidt, V.Z. Sun, A.R. Rodriguez, R. Tong, L. Tang, J. Cheng, T.J. Deming, D.T. Kamei, G.C. Wong, Translocation of HIV TAT peptide and analogues induced by multiplexed membrane and cytoskeletal interactions, Proc. Natl. Acad. Sci. U.S.A. 108 (2011) 16883–16888.
[35] A. Hoenger, J. McIntosh, Probing the macromolecular organization of cells by electron tomography, Curr. Opin. Cell Biol. 21 (2009) 89–96.
[36] F. Bertorelle, C. Wilhelm, J. Roger, F. Gazeau, C. Ménager, V. Cabuil, Fluorescence-modified superparamagnetic nanoparticles: intracellular uptake and use in cellular imaging, Langmuir 6 (2006) 5385–5391.
[37] B.G. Nair, Y. Nagaoka, H. Morimoto, Y. Yoshida, T. Maekawa, D.S. Kumar, Aptamer conjugated magnetic nanoparticles as nanosurgeons, Nanotechnology 21 (2010) 455102.